ELSEVIER

Journal of Power Sources 104 (2002) 24–32

JOURNAL OF POWER SOURCES

www.elsevier.com/locate/jpowsour

Parametric studies of a double-cell stack of PEMFC using Grafoil™ flow-field plates

J.-J. Hwang*, H.-S. Hwang

Department of Mechanical Engineering, Chung-Hua University, Hsinchu 300, Taiwan, ROC

Received 21 May 2001; accepted 18 July 2001

Abstract

A parametric study of a double-cell stack of a proton exchange membrane fuel cell (PEMFC) using Grafoil™ flow-field plates is performed. A self-made membrane–electrode assembly (MEA) is used to integrate the PEMFC. Emphasis is placed on the effect of the transport parameters such as cell temperature, pressure and humidity of the reaction side, and flow-field geometry on the performance of the stack. Potential–current and power–current curves are presented. At a fixed dew point of the incoming reactants, say $T_{dp} = 30\ ^{\circ}C$, increasing the cell operating temperature past a threshold value of about 50 °C reduces the cell performance due to membrane dehydration. At a fixed cell operating temperature, a high flow back-pressure increases the cell performance through enhancing the reaction on both electrodes of the fuel cell. Moreover, the cell performance for the pressurised cathode side is better than that for the pressurised anode side due to the favourable back-diffusion of water in the membrane. Finally, empirical correlations are developed to describe the electrode process of the PEMFC stack under various operating conditions.

Keywords: Proton exchange membrane; Fuel cell; Grafoil™; Dew point; Back-pressure; Performance

1. Introduction

Due to the limitation of fossil-fuel resources and environmental concerns, it is imperative to look for new and cleaner ways to produce and use energy. The fuel cell offers a means to produce high-efficiency electricity without harmful emissions. It converts chemical energy directly into electrical energy and offers a much better efficiency than most existing energy-conversion devices. In addition, when fuel systems of hydrogen/oxygen or hydrogen/air are used, the fuel cell is totally pollution free. Among the various existing fuel cell systems, the proton exchange membrane fuel cell (PEMFC) is the most promising, especially for terrestrial applications such as power generation and transportation, because of its simplicity in design and operation. Some other attractive characteristics of the PEMFC system include CO_2 tolerance, self-starting at low-temperature, no electrolyte leakage problems, and low-cost construction materials.

During the past two decades, the research and development of the PEMFC with a Nafion® membrane as electrolyte has received much attention. Much research has focused on single-cells of PEMFC or their components, such as novel membrane electrolytes [1,2], catalysts and structure [3], electrochemical reaction mechanisms and kinetics [4], as well as electrode materials and preparation [5,6]. For the fabrication of current-collector (flow-field) plates for the fuel cell, a variety of metal and non-metal materials such as stainless steel, titanium, aluminium and graphite have been used. In general, a fuel cell constructed from the graphite is resistant to corrosion but suffers from being brittle, and is expansive, bulky and difficult to machine. Recently, flexible graphite (this paper discusses the use of Grafoil™), which is used in high-temperature gaskets, has been used to fabricate the flow-field plate of the fuel cell. It is electrically conducting, corrosion resistant, and self-sealing, which obviates the requirement for separate gaskets. A previous single-cell study has revealed that Grafoil™ offers significant gains in performance over standard graphitic materials due to its compressibility that enables it to form an intimate contact with the electrode and minimise the interfacial resistance [7]. Due to the weakness in mechanical strength, however, it is questionable whether a stack using Grafoil™ for the flow-field plates can provide the same performance as that of a single-cell. Therefore, before building a multiple-cell stack for high-power application, it is important to determine the performance of a double-cell stack using Grafoil™ flow-field plates. In this study, we access the performance of a

* Corresponding author. Tel.: +886-3537-4281/8334; fax: +886-3537-3771.
E-mail address: jjhwang@chu.edu.tw (J.-J. Hwang).

0378-7753/02/$ – see front matter
PII: S0378-7753(01)00865-5

double-cell stack of PEMFC using Grafoil™ flow-field plates. Emphasis is placed on examining the effect of cell operating parameters such as cell temperature, dew point of the incoming reactants, flow-field pressure, and flow-field geometry on the fuel cell performance. A self-made membrane–electrode assembly (MEA) is used to integrate the double-cell stack of PEMFC. Empirical correlations are developed to describe the electrode process of the double-cell stack of PEMFC under various operating conditions. It is believed that the results obtained in this study can construct a bridge between the development of a high-power PEMFC stack using Grafoil™ as current-collectors and its use in portable and transportation applications.

2. Experimental apparatus

2.1. Apparatus

A schematic drawing of the experimental apparatus employed in the present study is shown in Fig. 1. It consists of a double-cell PEMFC stack and a test station (Globe Tech Inc.) together with a data-acquisition system. The test station provides the reactants (air and fuel) and controls the electric load while the data-acquisition system measures and records the required information. The measurement conditions are set using a PC and an associated software program. Both air and fuel streams are saturated by passing through water bottles before entering the fuel cell. The water bottles are maintained at a chosen temperature via a temperature-controller. The gas connections between the gas-control system and the fuel cell inlets are well insulated to prevent the water vapour from cooling and condensing on the way to the fuel cell. From the fuel cell outlets, the remaining fuel flows back to the gas-control system, while the air exits to the atmosphere. The back-pressure of the flow-fields in the anode and cathode is adjusted by regulators. The fuel cell is connected to an electronic load, which can be used in a constant current, voltage or power mode.

2.2. MEA and cell module

The MEA, a key component of a PEMFC system, is a proton-conducting membrane laminated between the active sites of two electrodes. In the present study, the proton-conducting membranes used are Nafion® 105. They are prepared by the following process. First, the membranes are soaked in a mixture of H_2O_2/H_2O at approximately 30 °C for 2 h and then are washed with distilled water to remove organic and mineral impurities. Next, the transparent Nafion® membranes are soaked in 1 M boiling H_2SO_4 solution for 2 h. Finally, they are rinsed again to remove excess H_2SO_4 and, being ready to use, are stored in distilled water. Subsequently, the commercially available electrocatalyst, 20% platinum on Vulcan XC-72 carbon (from E-Tek), is suspended in an aqueous Nafion® solution, which is then well mixed by using an ultrasonic bath. The resulting mixture is then printed directly on both sides of the membrane as active layers, rather than deposed on to diffusion layers (carbon paper) The amounts of Pt and Nafion® on the

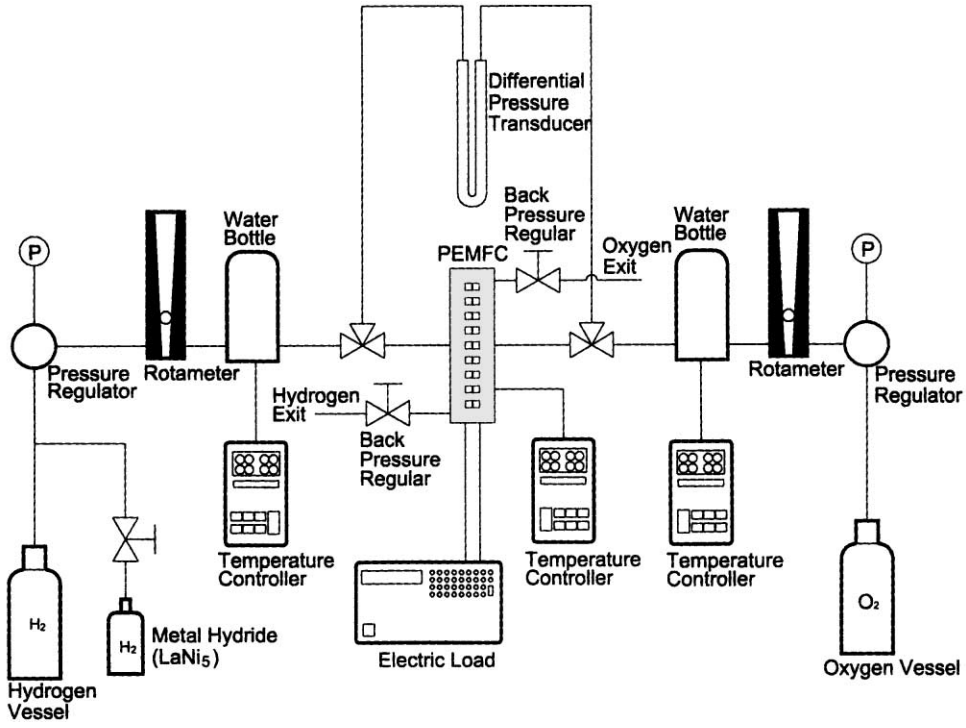

Fig. 1. Schematic of experimental apparatus.

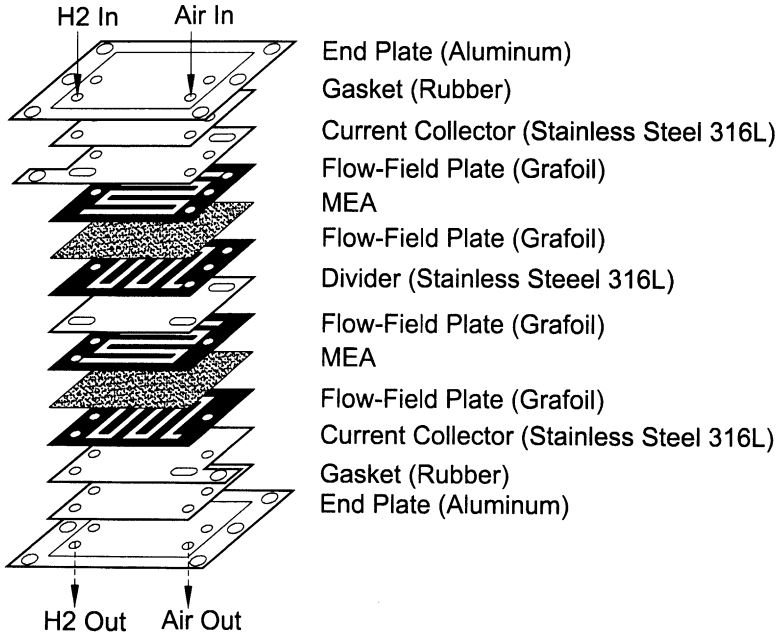

Fig. 2. Detailed structure of double-cell stack of PEMFC.

electrode were about 0.2 and 0.6 mg cm^{-2}, respectively For both electrodes, diffusion layers composed of 20% Pt/C and 0.378 mg cm^{-2} Pt are added to the carbon clothes. The electrode/membrane/electrode is assembled conventionally, using a hot-pressing process conducted at 140 °C and 8 MPa (about 1200 psi) for 90 s, in which the electrode/membrane/electrode laminate is heated until the glass transition temperature of the membrane is reached. The active surface area of the MEA is 25 cm^2.

Fig. 2 shows the detailed construction of the double-cell stack of PEMFC. The flow-field plates made from 2 mm thick Grafoil™. A serpentine flow configuration consists of sets of parallel flow channels arranged in series. The channel configuration of the baseline case for the present test is 1.5 mm^2 spaced by 1.5 mm, and is identical on the air and fuel sides. A stainless steel plate (316L) is sandwiched between two Grafoil™ flow-field plates to construct the bipolar plate. Two end-plates made of 10 mm thick aluminium are used to hold the MEA. Six screw rods around the perimeter of the end-plate are used to hold the stack. The stack has an internal manifold with the reactant gases (air and hydrogen) being delivered in one corner of the plate and removed from the opposite corner. A moment wrench was used to ensure that the electrical contact between the cell components was same in every measurement.

2.3. Experimental conditions

In the present study, potential curves are measured under various cell temperatures, dew points of the gases, back-pressure of the gas in the flow-field, and flow-field geometry to examine their effects on the fuel cell performance. The test conditions in the present study are shown in Table 1. Pure hydrogen (99.99% H_2) and air are used for the reactant gases in anode and cathode sides, respectively. H_2 and air are fed at 150 and 200% of the stoichiometric requirements at the maximum current density. For tests of the membranes under high humidification conditions, passing these gases through temperature-controlled water bottles (Fig. 1) humidifies the gasses and controls their dew points before entering the fuel cell. In addition, a ceramic heater together with a turbofan connected to a micro-switch is used to control the cell operating temperature. The cells are heated to a constant temperature in the range 30–80 °C by inserting a ceramic heater into the end-plate. To monitor the internal temperature of the stack, a copper–constantan thermocouple (T-type) is positioned inside the stack. To keep the cell temperature at a constant value, the micro-switch is triggered automatically to control the heater/fan when the temperature is lower/higher than the required value by 2 °C. In general, the double-cell stack has a good heat exchange and, therefore, the entire stack can be considered a lump system with the same temperature. The variables measured include temperature, pressure, flow rate, inlet air humidity, current, cell potential, and stack voltage.

Table 1
Test conditions of present study

Cell operating temperature T_c (°C)	30–80
Dew point of reactants T_{dp} (°C)	30–80
Back-pressure of the flow-field (atm)	1–3
Track dimension (mm)	1.5–3

3. Results and discussion

3.1. Effect of cell operating temperature

The effect of the cell operating temperature (30 °C $\leq T_c \leq$ 80 °C) on the performance of the present cell stack is shown in Fig. 3. The symbols and curves represent the results of potential–current and power–current relationships, respectively. Both streams of hydrogen and air are externally humidified with a dew point of $T_{dp} = 30$ °C before entering the fuel cell. That is, the amount of the vapour contained in the reactants is fixed. In order to obtain reproducible results, each experiment is conducted after the cell temperature has been equilibrated for at least 1 h.

For all the cell operating temperatures shown in Fig. 3, the potential–current curves have an initial rapid voltage drop at a very small current range due to an electrochemical activation process, which is caused by the sluggish kinetics of oxygen reduction at the cathode electrode surfaces [8]. Then, the Ohmic polarization controls the remaining part of the curve, in which the potential decreases linearly almost with increasing current density. There is no evidence of mass-transport limitations in the polarization curves shown in Fig. 3. In order to illustrate clearly the cell temperature effect, the cell potential is plotted in Fig. 4 as a function of the cell temperature for current densities of 100, 200 and 300 mA cm^{-2} The dashed curve relative to the right-hand side ordinate represents the relative humidity of the reactant gases at the corresponding cell operating temperature. Since the dew point temperature of the incoming gases is fixed, the relative humidity decreases monotonically with increasing cell operating temperature. It is seen that at a fixed current density, the cell potential increases slightly with increasing cell operating temperature from $T_c = 30$ °C, then reaches a maximum value at $T_c = 50$ °C, and finally decreases as T_c further increases. This behaviour may be explained as follows. As the cell operating temperature increases from $T_c = 30$ °C the ionic conductivity of the Nafion® membrane is enhanced [9], which results in an enhancement in cell performance. In fact, this gain in cell performance will be slightly offset by the decrease in the reversible potential with increasing the temperature according to the Nernst equation. The best performance is obtained when the cell is operated at a temperature of $T_c = 50$ °C, in which the relative humidity of the reactant gases is about 37%. For cell temperatures higher than $T_c = 60$ °C, the cell potential curve declines. Under cell operating temperatures of 70 and 80 °C, the relative humidity of the incoming reactants is severely low, typically only about 14.7 and 9.7%, respectively. In this situation, the amount of water vapour in the reactants in addition to the water production in the cathode side is insufficient to keep the membrane in a good hydrated condition. The membrane is, thus, dehydrated, resulting in a reduction of ionic conductivity and, subsequently, degradation of the cell performance [10]. It is concluded from the above results that with a fixed dew point ($T_{dp} = 30$ °C) of incoming reactants increasing the cell operating temperature from $T_c = 30$ to 80 °C has two major counteractive effects on the cell performance, namely, an increase in the ionic conductivity of membrane that enhances the cell performance [9] and dehydration of the membrane that deteriorates the cell performance. Thus, in the present study, increasing cell operating temperature past a threshold temperature of $T_c = 50$ °C causes membrane dehydration and, consequently, decreases cell performance.

It is worthy to note that the best operating conditions in the present study are very close to those reported by Murphy et al. [11]. In the latter work, the cell was operated at three different

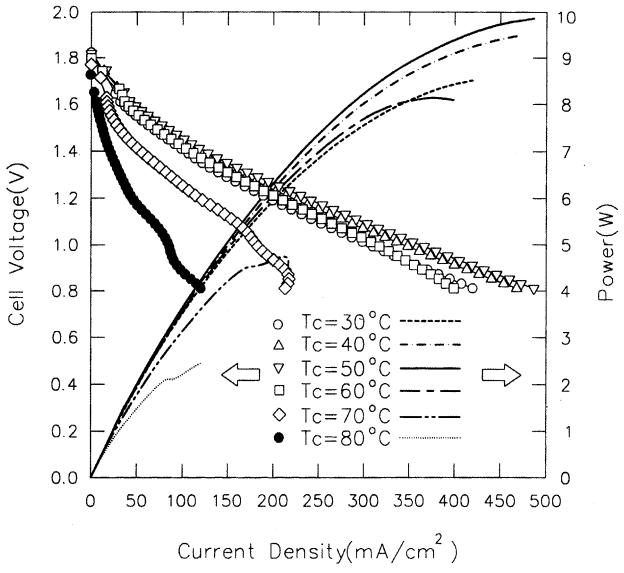

Fig. 3. Effect of cell operating temperature on cell performance at fixed dew point of reactants $T_{dp} = 30$ °C.

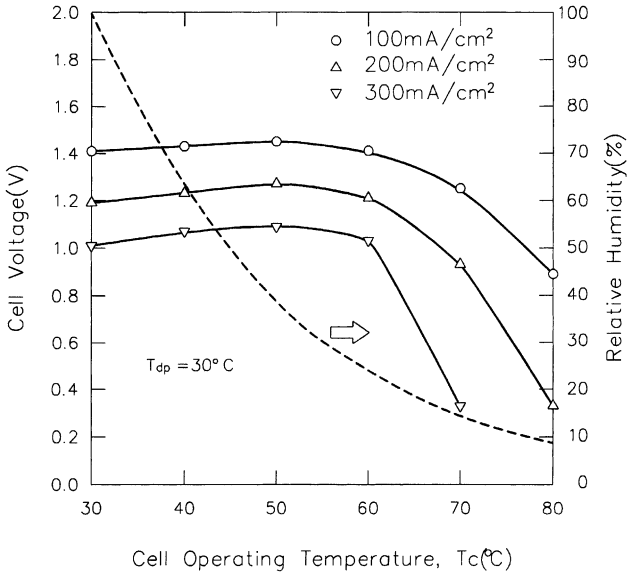

Fig. 4. Cell voltage as function of operating temperature at several current densities.

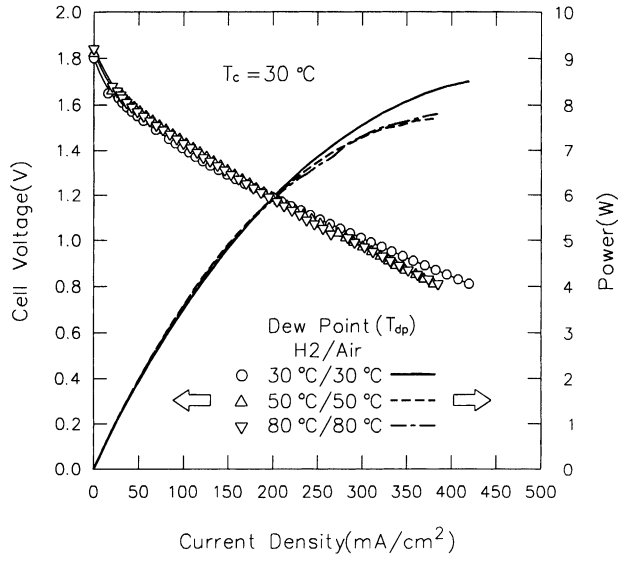

Fig. 5. Effect of dew point of reactants on cell performance at cell operating temperature $T_c = 30$ °C.

temperatures of $T_c = 46$, 62 and 71 °C and both gases were humidified at a dew point of $T_{dp} = 27$ °C. The best cell performance was obtained with the conditions of $T_c = 62$ °C and $T_{dp} = 27$ °C (with relative humidity about 30%).

3.2. Effect of dew point of reactants

The effect of the dew point of the hydrogen/air streams on the performance of the fuel cell under operating temperatures of $T_c = 30$ and 80 °C is shown in Figs. 5 and 6, respectively. In both cases, the dew points of both gas streams are varied together from $T_{dp} = 30$ to 80 °C to determine the optimum humidification conditions for the cell stack.

It is known that increasing the dew point temperature of the gases can increase the partial pressure of the vapour in the gas–vapour mixture and, thus, can increase the vapour mass flux in the flow-field. Typically, the partial vapour pressures are 4.25, 12.35 and 47.41 kPa, for $T_{dp} = 30$, 50 and 80 °C, respectively. At the low cell operating temperature of $T_c = 30$ °C (as shown in Fig. 5), the effect of the dew point temperature appears to be insignificant at a small current. In a high current density range (>250 mA cm^{-2}), however, humidification of the incoming gases to a dew point higher than the cell operating temperature is slightly detrimental to the cell performance, which may be due to flooding of the cell [12]. In general, a saturated but not flooded Nafion® membrane has the highest ionic conductivity [2]. Focus is now placed on the results for a fuel cell operated at the highest temperature of $T_c = 80$ °C (Fig. 6), in which the effect of dew point of the incoming reactants on the cell performance is quite significant. The results shown in Fig. 3 have revealed that the cell performance for the high operating temperature of $T_c = 80$ °C is rather poor at a dew point of $T_{dp} = 30$ °C due to severe dehydration of the membrane. When the dew point of the inlet gases is increased, the vapour volume flow in the gas flow-field is increased and dehydration of the membrane is less serious. Therefore, as shown in Fig. 6, on increasing the dew point up to $T_{dp} = 80$ °C, the fuel cell virtually maintains its own normal potential curve.

3.3. Effect of channel flow back-pressure

The effect of back-pressure of the flow-field in the anode and cathode channels on the performance of the fuel cell stack is shown in Figs. 7–9 for three different cell operating temperatures. Again, the gases for both air and fuel sides

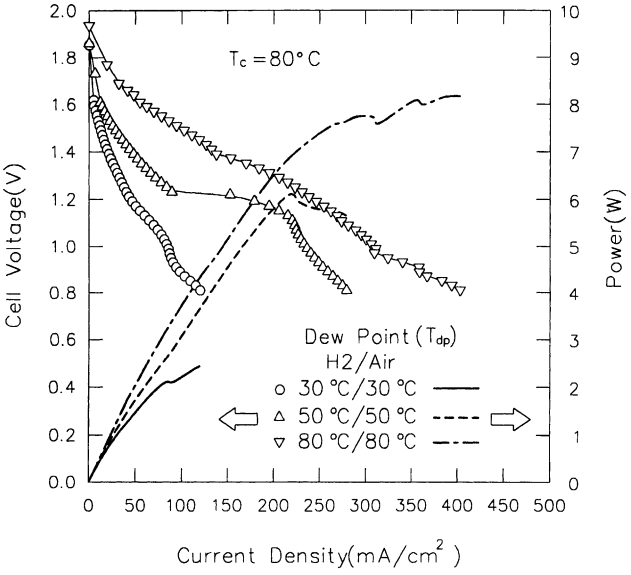

Fig. 6. Effect of dew point of reactants on cell performance at cell operating temperature of $T_c = 80$ °C.

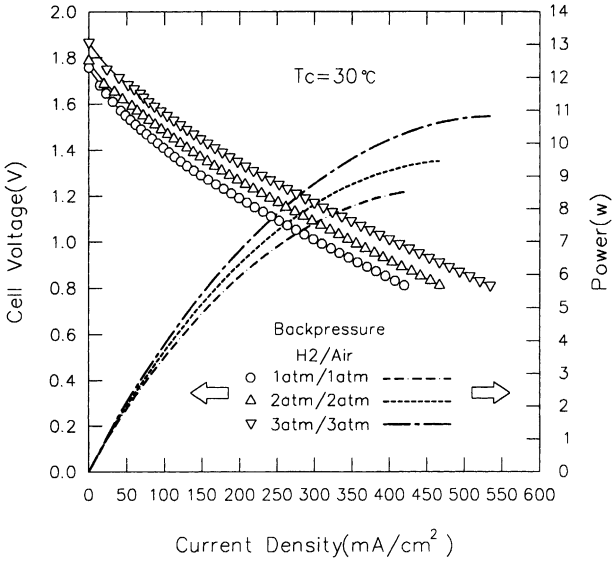

Fig. 7. Effect of back-pressure of flow-field on cell performance at $T_c = 30$ °C.

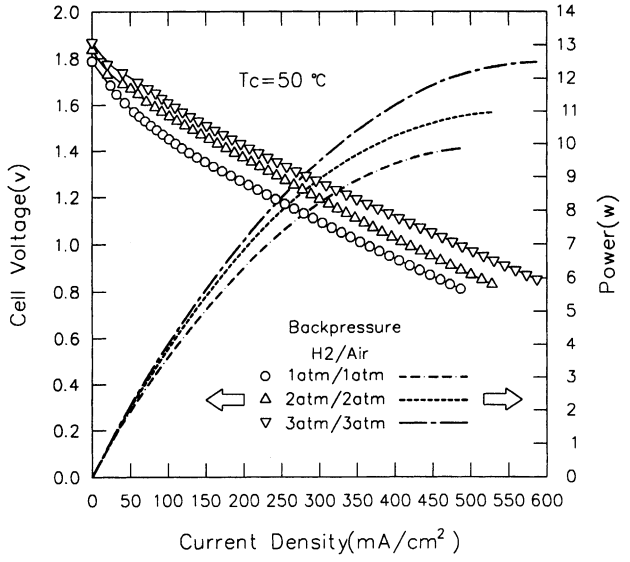

Fig. 8. Effect of back-pressure of flow-field on cell performance at $T_c = 50\ ^\circ C$.

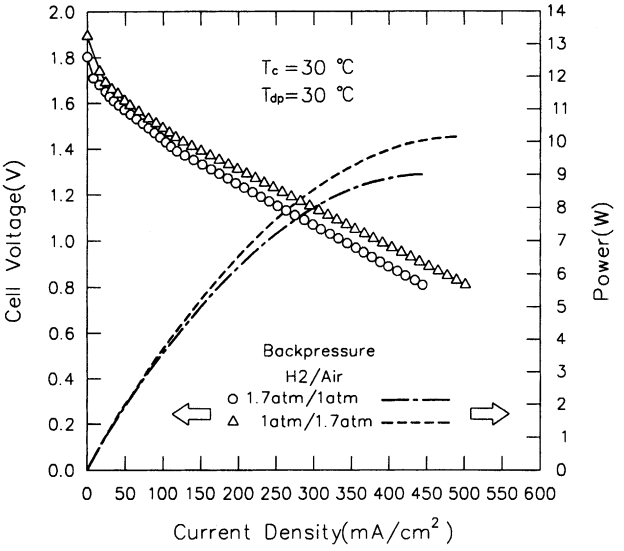

Fig. 10. Comparison of cell performance for asymmetrically pressurised flow-fields in anode and cathode sides.

are humidified at a dew point of $T_{dp} = 30\ ^\circ C$ before entering the fuel cell. The gas and fuel back-pressures are varied together from 1 to 3 atm, and are controlled by two regulators situated downstream in the gas flow exits (Fig. 1).

At a fixed cell operating temperature, the high back-pressure of the gas flow-field enhances the cell performance through enhancing the reaction at both electrodes of the fuel cell. In addition, according to the Nernst equation, an increase in oxidant pressure (air side) can increase the reversible cathode potential. Therefore, the general trend shown in Figs. 7 and 8 ($T_c = 30$ and $50\ ^\circ C$) is that increase in the back-pressure of the fluid flow can improve the cell performance. In contrast, at the highest cell operating temperature of $T_c = 80\ ^\circ C$ (Fig. 9), the improvement in the cell performance is believed to be the reason of the corresponding improvement in the hydrated conditions of the membrane. The enhancement in the reaction rate produces a large amount of water in the cathode side that can prevent dehydration of the membrane. That is, dehydration of the membrane at high-temperatures can be prevented by the pressurised operation.

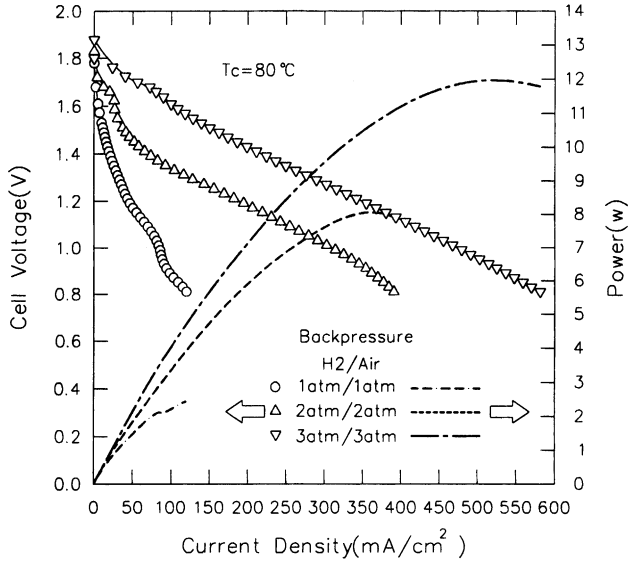

Fig. 9. Effect of back-pressure of flow-field on cell performance at $T_c = 80\ ^\circ C$.

The results of asymmetrically pressurised flow-fields in the cathode and the anode sides are shown in Fig. 10. The dew point of the incoming gases and the cell operating temperature are kept at $T_{dp} = 30\ ^\circ C$ and $T_c = 30\ ^\circ C$, respectively. It is seen that the cell performance for the pressurised cathode side (triangular symbols) is better than that for the pressurised anode side (circular symbols). The pressure difference across the membrane from the cathode side to the anode side is coincident with the direction of the back-diffusion of water in the membrane and, thus, enhances the back-diffusion effect to maintain a more ideal water distribution throughout the assembly. In addition, as mentioned above, increase in oxidant pressure can increase the reversible potential in cathode side. By contrast, as the back-pressure of the channel flow in the anode side is higher than that of the cathode side, the pressure gradient across the membrane adversely affects the back-diffusion of water to the hydrogen side and, thus, reduces the performance of the cell.

It should be noted that increasing the operating pressure increases the energy required to compress air and supply it to the stack. Therefore, the pressurising is a trade-off between increased power but a parasitic load and a more complicated system in practical fuel ell applications. The net benefit for

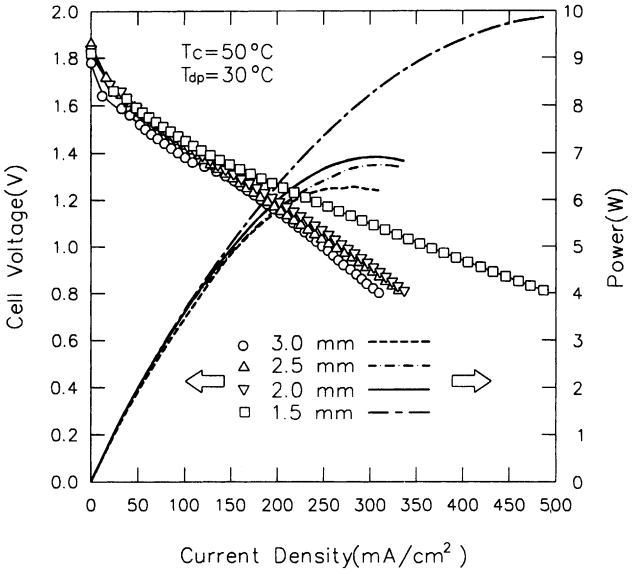

Fig. 11. Effect of channel dimensions on cell performance.

increasing the operating pressure of the fuel cell should be further evaluated.

3.4. Effect of flow channel dimensions

The effect of the gas channel dimensions on the cell performance under operating conditions of $T_c = 50\ ^\circ C$ and $T_{dp} = 30\ ^\circ C$ is presented in Fig. 11. In the present test, the width of the gas channels and current-collecting ribs is varied together, but their ratio is kept constant. It is seen that the cell performance is advantageous for geometry which reduces the channel/rib size. This may be explained as follows. At a fixed active area of the MEA, increasing the channel/rib width ensures a smaller total number of channel/ribs. Since the ribs in the flow-field are non-porous, the reactants must diffuse laterally through the backing to reach the catalyst in the regions beneath the ribs. Therefore, increasing rib width would increase the diffusion pathway and this, in turn, hinders gas diffusion through the electrode and renders areas of the cell inactive. The use of narrower ribs in the flow-field can minimise the diffusion pathway and, thus, improve the cell performance. The pressure drop across such a flow-field may, however, be more significant in that it increases the energy required to compress air and supply it to the stack.

3.5. Analysis of electrode kinetic and Ohmic parameters

According to the empirical equations developed by Kim et al. [13] and Rho et al. [14] to describe the electrode process for a single-cell of a PEMFC, the total potential of a double-cell stack of PEMFC assembled in series can be described as

$$E_i = E_o - b \log i - iR \quad (1)$$

$$E_o = E_r - b \log i_o \quad (2)$$

Table 2
Electrode kinetic parameters for PEMFC with Nafion® membranes as function of cell temperature, reactant dew point temperature, and flow-field pressure

Test condition	Cell temperature T_{dp} (°C)	Dew point of reactants T_{dp} (°C)	Gas pressure H_2/air (atm)	Tafel parameters		
				E_o (V)	b (mV)	R (Ω)
#1	30	30	1/1	1.822	72	0.070
	40	30	1/1	1.840	76	0.063
	50	30	1/1	1.842	86	0.052
	60	30	1/1	1.831	76	0.067
	70	30	1/1	1.730	87	0.094
	80	30	1/1	1.620	91	0.222
#2	30	30	1/1	1.842	58	0.077
	30	50	1/1	1.851	51	0.085
	30	80	1/1	1.873	61	0.082
	80	30	1/1	1.620	91	0.222
	80	50	1/1	1.571	108	0.093
	80	80	1/1	1.730	140	0.045
#3	30	30	1/1	1.842	58	0.077
	30	30	2/2	1.931	69	0.067
	30	30	3/3	2.031	75	0.063
	50	30	1/1	1.913	83	0.057
	50	30	2/2	1.922	39	0.065
	50	30	3/3	1.943	47	0.059
	80	30	1/1	1.620	91	0.222
	80	30	2/2	1.829	94	0.053
	80	30	3/3	1.959	56	0.055
#4	50	30	1.7/1	1.835	43	0.071
	50	30	1/1.7	1.903	81	0.049

where E_i and i are the experimentally measured stack potential and current, respectively; E_o the open-circuit potential of the stack; i_o and b the Tafel parameters for oxygen reduction; R the resistance (predominantly Ohmic) which causes a linear variation of the cell potential with current density and E_r is the reversible potential of the PEMFC. The electrode kinetic parameters of the present PEMFC stack obtained by fitting Eq. (1) at different operating conditions are summarised in Table 2. Several interesting conclusions which can be drawn from the data are as follows.

1. For test condition #1 (cell operating temperature effect), the smallest value of R for $T_c = 50\,^{\circ}C$ gives the best compromise in cell operating temperature and relative humidity of the reactants. In addition, the significantly high value of R for $T_c = 80\,^{\circ}C$ reflects the poor ionic conductivity of Nafion® membrane due to dehydration.
2. For test condition #2 (reactant dew point effect), the dew point of the incoming gases does not affect the above kinetic parameters too much at the low cell operating temperature ($T_c = 30\,^{\circ}C$). at the high cell operating temperature of $T_c = 80\,^{\circ}C$, however, the value of R is significantly reduced by increasing the dew point temperature from $T_{dp} = 30$ to $80\,^{\circ}C$.
3. For test condition #3 (back-pressure effect), the ionic conductivity of the membrane is improved by increasing the back-pressure of the flow-field, especially the high cell operating temperature. In addition, increasing the flow-field back-pressure increases the open-circuit voltage.
4. Under asymmetrically pressurised conditions (test condition #4), the higher back-pressure in the air side not only causes an improvement in ionic conductivity but also increases the open-circuit voltage.

4. Conclusions

A parametric study of a double-cell stack PEMFC using Grafoil™ flow-field plate has been performed. A self-made MEA with an active area of PEMFC is 25 cm^2 is used to integrate the PEMFC. The transport parameters of cell temperature ($30\,^{\circ}C \leq T_c \leq 80\,^{\circ}C$), reactant humidity ($30\,^{\circ}C \leq T_{dp} \leq 80\,^{\circ}C$), flow-field back-pressure (1 atm $\leq P \leq 3$ atm) and flow-field geometry (1.5, 2, 2.5, and 3 mm) have been examined. The cell performance for the pressurised cathode side is better than that for the pressurised anode side due to the favourable back-diffusion of water in the membrane. The main findings based on the experimental results are as follows.

1. Improving the cell performance through increase in temperature is limited the by high vapour pressure of water in the membrane due to the membrane susceptibility to dehydration and subsequent loss of ionic conductivity. Typically, at $T_{dp} = 30\,^{\circ}C$, increasing the cell operating temperature past a threshold value of about $50\,^{\circ}C$ reduces the cell performance due to membrane dehydration. The best cell performance is obtained at an operating temperature of $T_c = 50\,^{\circ}C$ along with a relative humidity of 34%.
2. At a fixed cell operating temperature, the high flow back-pressure increases the cell performance through enhancing the reaction both electrodes of the fuel cell. In addition, an increase in oxidant pressure (air side) can increase the reversible cathode potential.
3. The cell performance for the pressurised cathode side is better than that for the pressurised anode side. The pressure difference across the membrane from the cathode side to the anode side is coincident with the direction of the back-diffusion of water in the membrane and, thus, enhances the back-diffusion effect to maintain a more ideal water distribution throughout the assembly.
4. The electrode processes have been successfully analysed by an empirical equation that is fitted to the experimental polarization data at various operating conditions.

Acknowledgements

This work was sponsored by the National Science Council of the Republic of China under contract no. NSC 89-2212-E-216-003. In addition, the authors gratefully acknowledge the technical assistance of Dr. Y.C. Cheng, Asia Pacific Fuel Cell Technologies, Ltd.

References

[1] N. Yoshida, T. Ishisaki, A. Watakabe, M. Yoshitake, Characterisation of Flemion® membranes for PEFC, Electrochem. Acta 43 (1998) 2749.
[2] Y. Sone, P. Ekdunge, D. Simonsson, Proton conductivity of Nafion® 117 as measured by a four-electrode AC impedance method, J. Electrochem. Soc. 143 (1996) 1254.
[3] J. Fournier, G. Faubert, J.Y. Tuquin, R. Cote, D. Guay, J.P. Dodelet, High performance, low Pt content catalysts for the electroreduction of oxygen in polymer electrolyte fuel cells, J. Electrochem. Soc. l44 (1997) 45.
[4] D. Chu, O_2 reduction at the Pt/Nafion® interface in 85% concentrated H_3PO_4, Electrochem. Acta 43 (1998) 3711.
[5] K.Y. Chen, A.C.C. Tseung, Effect of Nafion® dispersion on the stability of Pt/WO_3 electrodes, J. Electrochem. Soc. 143 (1996) 2702.
[6] P.K. Shen, K.Y. Chen, A.C.C. Tseung, CO oxidation on Pt/Ru/WO_3 electrodes, J. Electrochem. Soc. 142 (1995) L85.
[7] P.L. Hentall, J.B. Lakeman, G.O. Mepstep, P.L. Adcock, New materials for polymer electrolyte membrane fuel cell current-collectors, J. Power Sources 80 (1999) 235.
[8] D. Chu, R. Jiang, J. Power Sources 80 (1999) 226.
[9] F.N. Buchi, G.G. Scherer, In situ resistance measurements of Nafion® 117 membranes in polymer electrolyte fuel cells, J. Electroanal. Chem. 404 (1996) 37–43.
[10] A.V. Anantaraman, C.L. Gardner, Studies on ion-exchange membranes. Part 1. Effect of humidity on conductivity of Nafion®, J. Electroanal. Chem. 414 (1996) 115–120.

[11] O.J. Murphy, A. Cisar, E. Clarke, Low-cost light weight high-power density PEM fuel cell stack, Electrochem. Acta 43 (1998) 3829.

[12] H.H. Voss, D.P. Wilkinson, P.G. Pickup, M.C. Johnson, V. Basura, Anode Water Removal: A Water Management and Diagnostic Technique for Solid Polymer Fuel Cells, Vol. 40, 1995, p. 321.

[13] J. Kim, S.M. Lee, S. Srinivason, C.E. Chamberlin, Modelling of proton exchange membrane fuel cell performance with an empirical equation, J. Electrochem. Soc. 142 (1995) 2670.

[14] Y.W. Rho, O.A. Velve, S. Srinivason, Y.T. Kho, Mass-transport phenomena in proton exchange membrane fuel cells using O_2/He, O_2/Ar, J. Electrochem. Soc. 141 (1994) 2084.